Microfluidic Chip Coupled with Modified Paramagnetic Particles for Sarcosine Isolation in Urine

Ondrej Zitka[1,2], Natalia Cernei[1], Zbynek Heger[1], Miroslav Matousek[1], Pavel Kopel[1,2], Jindrich Kynicky[2,3,4], Michal Masarik[2,5], Rene Kizek[1,2], Vojtech Adam[1,2*]

[1]Department of Chemistry and Biochemistry, Faculty of Agronomy, and [3]Department of Geology and Pedology, Faculty of Forestry and Wood Technology, Mendel University in Brno, Zemedelska 1, CZ-613 00 Brno, Czech Republic, European Union

[2]Central European Institute of Technology, Brno University of Technology, Technicka 3058/10, CZ-616 00 Brno, Czech Republic, European Union

[4]Karel Englis College, Sujanovo nam. 356/1, CZ-602 00, Brno, Czech Republic, European Union

[5]Department of Pathological Physiology, Faculty of Medicine, Masaryk University, Komenskeho namesti 2, CZ-662 43 Brno, Czech Republic, European Union

***Corresponding author**

Vojtech Adam, Department of Chemistry and Biochemistry, Mendel University in Brno, Zemedelska 1, CZ-613 00 Brno, Czech Republic, European Union; E-mail: vojtech.adam@mendelu.cz; phone: +420-5-4513-3350; fax: +420-5-4521-2044

Keywords: Ion Exchange Chromatography; Magnetic Nanoparticles; Microfluidic Separation; Prostate Cancer; Surface Modification

Total words count: 6277

List of abbreviations: CaP – Carcinoma of Prostate; GWAS – Genome-Wide Association Studies; PLA – Poly-Lactic Acid; PMPs – Paramagnetic Particles

Received: March 3, 2013; Revised: May 8, 2013; Accepted: May 9, 2013

This article has been accepted for publication and undergone full peer review but has not been through the copyediting, typesetting, pagination and proofreading process, which may lead to differences between this version and the Version of Record. Please cite this article as doi: 10.1002/elps.201300114.

Abstract

Carcinoma of prostate (CaP) is the second most frequent malignant tumour occurring in men in Europe. Currently there is discussed a wide range of potential CaP markers. One of them – non/protein amino acid sarcosine, also known as N-methylglycine was chosen as a challenge for the development of microfluidic system with isolation by modified paramagnetic microparticles (PMPs). Therefore, the aim of this study was to design a low-cost, simple and rapid microfluidic system based on sarcosine isolation with modified paramagnetic microparticles and subsequent analysis on the ion-exchange liquid chromatography. We modified Dowex microparticles with Fe_2O_3 nanoparticles. Our paramagnetic microparticles were able to establish the binding with sarcosine. Moreover, we designed microfluidic device for sarcosine determination. Analysis of samples was carried out with limit of detection of 1 μM of a sarcosine that is sufficient because it is similar to concentrations of a sarcosine observed in the CaP patients.

1 Introduction

Genome-wide association studies (GWAS) revealed links between genetic variance and predisposition to disease. With the advent of modern 'omics-technologies', GWAS can now identify the genetic factors that influence intermediate traits on pathways to disease, such as blood concentrations of carbohydrates, lipids, amino acids, and secondary metabolites, hormones and signal molecules [1-4]. Increasing interest about sarcosine as of the secondary metabolites is dated from year 2009, when Sreekumar et al. published their study, which provided new information about possible utilization of sarcosine as a potential prostate carcinoma marker [5]. Sarcosine is CH_3NHCH_2COOH formulated as a natural, colourless, non-toxic and solid substance well soluble in water. Sarcosine, also N-methylglycine is methyl derivate of glycine, created in organism as an intermediate metabolic products generated during conversion of choline to glycine [6]. Although the connection of sarcosine with amino acids metabolism and methylation processes of prostate tumours progression was described [7-9] as well as its potential in a diagnosis of early stages of prostate tumours [10, 11], usage as a marker is still under discussions, because there can be found some publications that disproved link between sarcosine and prostate tumours [12]. On the other hand, sarcosine is not present in urine of health people, therefore, false positivity is minimized [13, 14]. Recently, numerous methods are developed for sarcosine detection. Most of them are based on different types of chromatography or capillary electrophoresis (CE) or microfluidic chips [15-19] coupled mainly with mass spectrometry [7, 20-28]. There is also possibility to couple modern separation methods with electrochemical detectors, which have low operating costs, the possibility of miniaturization and high sensitivity [29, 30]. Direct electrochemistry using modified glassy carbon electrode was applied by Zhou et al. for sarcosine oxidase detection and detection limits were estimated as 1 μM [31].

In our study we decided to use ion exchange chromatography with post-column ninhydrin derivatization and VIS detector for sarcosine separation and detection, which minimizes the sample pre-treatment requirements [13]. Major part of the study consisted of sarcosine isolation by Dowex 50WX4-400 microbeads with SO_3^- functional groups. Surface was modified by paramagnetic particles (PMPs), which are formed by Fe_2O_3 nanoparticles. Magnetic particles can combine two selective processes in bioanalysis: the specific binding of analytes to the particle surface based on molecular recognition and the specific isolation of magnetic objects from complex sample mixtures [32]. Possibility of MPs surface modification and thereby an elimination of undesirable biomolecules adsorption is the biggest advantage of their utilization [33, 34]. The obtained partially modified surface of our Dowex magnetic particles was characterized by electron microscopy. Application of nanoparticles for isolation of sarcosine was carried out in reaction cell fabricated using 3D printer.

2 Materials and methods

2.1 Chemicals and pH measurement

Working solutions as buffers or standard solution of sarcosine were prepared daily by diluting the stock solutions (110 mM), which were stored in refrigerator at 4 ^oC. Sarcosine standards and others were purchased from Sigma Aldrich (St. Louis, Missouri, USA) in ACS purity (chemicals meet the specifications of the American Chemical Society), unless noted otherwise. Washing solutions were prepared in MiliQ water obtained using reverse osmosis equipment Aqual 25 (Aqual s.r.o., Brno, Czech Republic). The deionised water was further purified by using apparatus Direct-Q 3 UV Water Purification System equipped with the UV lamp from Millipore (Billerica, Massachusetts, USA). The resistance was established to 18 $M\Omega.cm^{-1}$. The pH was measured using pH meter WTW inoLab (Weilheim, Germany).

2.2 Preparation of nanoparticles

Maghemite nanoparticles were prepared by sodium borohydride ($NaBH_4$) reduction of iron chloride ($FeCl_3.6H_2O$) according to Magro et al. and Prucek et al. [35, 36]. Briefly, 1 g of $FeCl_3 \cdot 6H_2O$ was dissolved in 80 mL of MilliQ water and a solution of 0.2 g of $NaBH_4$ in ammonia (10 mL, 3.5% *m/v*) was poured into the first solution with vigorous stirring. The evolution of hydrogen was observed and mixture turned to brick red. The obtained solution was heated at boiling temperature for 2 h. After cooling and standing for 2 h at room temperature, the obtained magnetic nanoparticles were separated by external magnetic field and washed several times with water. The nanoparticles, prepared as described above were suspended in 80 mL of water and 0.5 g of Dowex 50WX4-400 (Sigma Aldrich) was added. The mixture was shaken for 12 h at room temperature and after that separated by external magnetic field and washed several times with water. Product was dried at 50 ºC. The synthesized paramagnetic particles (PMPs) were prior to use after dilution.

2.3 SEM characterisation of Dowex modified microparticles

Structure and elemental composition of paramagnetic microparticles were characterised by electron microscope. For documentation of the selected nanomaterials a FEG-SEM MIRA XMU (Tescan, a.s., Brno, Czech Republic) was used. This model is equipped with a high brightness Schottky field emitter for low noise imaging at fast scanning rates. The SEM was fitted with Everhart-Thronley type of SE detector, high speed YAG scintillator based BSE detector, panchromatic CL Detector and EDX spectrometer. The MIRA 3 XMU system is based on a large specimen chamber with motorized stage movements 130×130 mm. Samples were coated by 10 nm of carbon to prevent sample charging. A carbon coater K950X (Quorum Technologies, Grinstead, United Kingdom) was used. For automated acquisition of selected areas a TESCAN proprietary software tool called Image Snapper was used. The

software enables automatic acquisition of selected areas with defined resolution. Different conditions were optimized in order to reach either minimum analysis time or maximum detail during overnight automated analysis. An accelerating voltage of 15 kV and beam currents about 1 nA gives satisfactory results regarding maximum throughput.

2.4 Electrochemical microscope

Identification of relative current response before and after sarcosine binding to PMPs was obtained by scanning electrochemical microscope Model 920D (CH instruments, Inc. USA). Electrochemical microscope consisted of 10 mm measuring platinum disc probe electrode with potential of 0.2 V. Another platinum disc electrode with O-ring as conducting substrate used potential of 0.3 V. During scanning, the particles were attached on the substrate platinum electrode by magnetic force from neodyme magnet, which was situated below the electrode. Platinum measuring electrode was moving from 150 µm above the surface. The scanning was carried out in the solution according Liljeroth et al. and Wittstock et al. [37, 38]. The mixture consisted of 5% ferrocene in methanol (*m/v*) mixed in ratio 1:1 with 0.05% KCl in water (*v/v*). Measuring was performed in Teflon cell with volume of 1.5 mL according to the following parameters: amperometric mode, vertical scan was carried out in area 500 × 500 µm with scan rate 30 $\mu m.s^{-1}$.

2.5 Fabrication of the reaction cell in microchip

Reaction cell was designed in Blender software (NetFabb Studio, USA) and manufactured under laboratory conditions using 3D printer Easy 3D Maker (3DFactories, Straznice, Czech Republic). The printing material was biodegradable polymer poly-lactic acid (PLA). A distinct advantage of using polymers is the fact that materials with specific chemical and physical properties (such as optical transparency, chemical resistance, stiffness, critical

surface tension, etc.) can be selected specifically for a target application [39]. The time of printing was 30 minutes while the density of the matrix was set on 100 %. The pad for the target was tempered on 35 °C.

2.6 Sample preparation

PMPs stock solution consisted of 40 mg PMPs in 1,000 µL of water with ACS purity and was treated with ultrasonic homogenizer SONOPULS mini20 (Bandelin electronic, Berlin, Germany) for 2 minutes. Then, diluted 50 µL of PMPs were mixed together with 200 µL of PBS prior to further experiments. After steps conducted in chip mentioned in chapter 2.4, mixture of Britton-Robinson buffer and sarcosine bound on PMPs was eluated from chip to an Eppendorf tube, where eluate was discarded with permanent magnet purchased from Chemagen (Baesweiler, Germany). Retentate consisting of PMPs with sarcosine was dissolved in 3 M HCl and incubated at room temperature for 15 minutes with 1250 rpm in thermoblock Thermomixer® R (Eppendorf AG, Hamburg, Germany). Dissolved PMPs were transferred to 96-well evaporation plate Deepwell plate 96 (Eppendorf AG, Hamburg, Germany) and evaporated. For evaporation of dissolved PMPs the nitrogen blow-down evaporator Ultravap 96 with spiral needles (Porvair Sciences limited, Leatherhead, United Kingdom) was used. The prepared sample was ready for analysis at ion-exchange chromatography.

2.7 Ion exchange chromatography

For determination of sarcosine an ion-exchange liquid chromatography (Model AAA-400, Ingos, Prague, Czech Republic) with post column derivatization by ninhydrin and absorbance detector in visible light range (VIS) was used. Glass column with inner diameter of 3.7 mm and 350 mm length was filled manually with strong cation exchanger (Ostion LG ANB,

Ingos, Prague, Czech Republic) in sodium cycle called with approximately 12 μm particles and 8% porosity. Column was tempered at 60 °C. Double channel VIS detector with inner cell of 5 μL was set to two wavelengths: 440 and 570 nm. Solution of ninhydrin (Ingos) was prepared in 75% methylcelosolve (*v*/*v*, Ingos) in 2% (*v*/*v*) 4 M acetic buffer (pH 5.5). Tin chloride ($SnCl_2$) was used as a reducing agent. Prepared solution of ninhydrin was stored under inert atmosphere (N_2) in dark at 4 °C. Elution of sarcosine was done by buffer containing 10.0 g of citric acid, 5.6 g of sodium citrate, and 8.36 g of NaCl per litre of solution and pH was 3.0. Flow rate was 0.25 $mL.min^{-1}$. Reactor temperature was set on 120 °C. For dilution of samples the diluting buffer was used (composition: Thiodiglykol 41 mM, citric acid 67 mM, sodium chloride 0.2 M). Other experimental conditions are in the following papers [13, 40].

2.8 Artificial urine and urine samples

To 1.5 litres of distilled water, 36.4 g of urea, 15.0 g of sodium chloride, 9.0 g of potassium chloride, 9.6 g of sodium phosphate 4.0 g of creatinine and 100 mg of albumin were added. pH of the artificial urine was 6. Besides artificial urine, we also analysed urine samples obtained from laboratory stuff (10 men). Age of people ranged from 18 to 25 years (mean 22.4 years). Urine of the stuff was centrifuged at 4,000 g for 10 min (Eppendorf 5402, USA). The samples were stored at -20 °C prior to analysis.

2.9 Recovery

Recovery of sarcosine determination was evaluated with urine spiked with standard with concentration of 1.1 mM. Before extraction, 100 μL sarcosine standards and 100 μL water were added to urine samples. Urine was assayed blindly and sarcosine concentrations were derived from the calibration curve. The spiking of sarcosine was determined as a standard

measured without presence of real sample. Calculation of recovery was carried out as indicated by Causon [41] and Bugianesi et al. [42].

2.10 Descriptive statistics

Mathematical analysis of the data and their graphical interpretation were realized by Microsoft Excel®, Microsoft Word® and Microsoft PowerPoint®. Results are expressed as mean ± standard deviation (S.D.) unless noted otherwise. The detection limits (3 signal/noise, S/N) were calculated according to Long and Winefordner [43], whereas N was expressed as standard deviation of noise determined in the signal domain unless stated otherwise.

3 Results and discussion

Isolation of the low molecular mass molecules based on the adsorption on the beads with various modifications is the major idea of the liquid separation techniques as liquid chromatography using filled columns. To develop the magnetic separation based on chip fluidic system we wanted to create micro ion exchanger for specific isolation of sarcosine, as we reported before that standard ion exchange chromatography was useful for this purpose [13]. Due to the combination of the selective isolation based on the paramagnetic particles it is possible to implement this technology into the microfluidic chip with continuous flow.

3.1 Dowex modification

As primary platform for ion exchange separation we used commercially available Dowex substrate which is based on the silica particles in diameter of tens micrometres. These particles were modified according to the protocol mentioned in section 2.2. Picture of paramagnetic microparticles, which we modified, is shown in Fig. 1Aa, where small differences in Dowex surface coverage with Fe_2O_3 cane be observed. This effect may be

caused by sample pre-treatment before scanning by electron microscope. Detail of one PMP is shown in Fig. 1Ab. Most important parts of PMPs are Fe_2O_3 nanoparticles and SO_3^- functional groups. The magnetic properties of our particles are provided by Fe_2O_3 nanoparticles that are spread over the surface of Dowex bead, as can be seen in Fig. 1Ac, where iron from the paramagnetic particles is red highlighted. SO_3^- functional groups that mediate binding of sarcosine and are partly covered with Fe_2O_3 nanoparticles are orange highlighted (Fig. 1Ad).

We also acquired the scans of current response of PMPs with or without sarcosine on the surface with scanning electrochemical microscope. The scan of the surface without sarcosine is shown in Fig. 1Ba. There are reported periodic differences in surface current response due to unbound SO_3^- functional groups. After establishing of sarcosine-PMPs binding the change of surface current response was determined (Fig. 1Bb). The stabilization of relative current response occurred because of decrease of binding positions for coupling of amino acids.

3.2 Fluidic chip based experimental design

After that we characterized particles used in this study, all experiments were carried out using microfluidic separation in our manufactured design of microchip with overall working volume 500 µL (Figs. 2A-G). The outlet for the syringe with volume 10 mL (B. Braun Melsungen AG, Melsungen, Germany) was used for dosing of the solutions into the chip. All experiments conducted with a chip instead of dissolution of retentate in HCl, evaporation and VIS detection were held in refrigerated room with optimized temperature as 10 ºC. Workflow ongoing in refrigerated room consisted of three times washing of PMPs with PBS buffer and three times washing of PMPs with Britton-Robinson buffer. Washing was performed with 5 mL of each buffer. As the following step, the incubation was carried out for 5 minutes at 10

ºC. After incubation, another washing step using three times Britton-Robinson buffer was included.

The entire process of our workflow is shown in Fig. 3A. It was necessary to include washing steps. In study by Zhang et al., water and ethanol were used for removing of excess reagents [44]. In our study particles were washed with PBS and Britton-Robinson buffer to remove undesired particles of impurities from beads because of the differences in the nature of particles and need of maintaining low pH, which showed the highest yields in the optimization. Then binding of sarcosine to beads via SO_3^- functional groups was established that exhibited the affinity with molecules like amino acids, where the protonated amino-group has the same order of ion exchange selectivity [45]. To achieve optimal binding, there was an incubation included, which was carried out according to the optimized conditions mentioned in chapter 3.3. After proper incubation, eluate was discarded with the permanent magnet and remaining solid material after removal of the eluate containing the bound sarcosine on PMPs was dissolved in 3 M HCl after applying of additional three washing steps using Britton-Robinson buffer pH 2. HCl dissolution was performed in Eppendorf tubes due to the adverse effects of HCl to the material, from which the chip was crafted. Through this, the particles with bound sarcosine were dissolved and prepared for the evaporation by nitrogen evaporator. Subsequent analysis using automatic amino acid analyser was performed after resuspension of evaporated retentate with dilution buffer to evaluate the whole separation protocol.

3.3 Optimization of sarcosine isolation

The effects of pH, time of adsorption, incubation temperature and dose of PMPs on the sarcosine amount bound to the beads were investigated (Figs. 3B-F). All optimization experiments were carried out with sarcosine standard with concentration 1.1 mM. All results

obtained as peak areas from VIS detection were converted to percentages for clearer interpretation of the optimization parameters effects.

3.3.1 Optimization of pH

Acidic pH maintained by Britton-Robinson buffer washing was proved as an essential parameter for establishing sarcosine-PMPs binding. As it is shown in Fig. 3B, the lowest selected pH 2 showed the highest amounts of bound sarcosine. The experiment was not conducted at lower pH than 2 because of occurrence of the unwanted dissolution of PMPs. With the increasing pH there was determined significant reduction of the sarcosine amount bound to beads (Fig. 3B). The highest tested pH was pH 4, but there was detected minimal amount of sarcosine bound. pH influence was probably caused by sorbent surface changes that revealed SO_3^- functional groups with decreasing pH, because the particles were partially covered with Fe_2O_3. Echigo et al. examined the effects of various parameters on hematite nanoparticles (Fe_2O_3) and indicates that pH buffers may cause their dissolution [46].

3.3.2 Optimization of the time of incubation

Effect of incubation time was evaluated at 1, 5, 10, 15, 30 and 60 minutes (Fig. 3C). A good dispersion of sorbent should considerably increase the contact surface area between the sorbent and analyte in sample leading to a higher adsorption efficiency and faster extraction time [3]. In ion exchange, the stationary phase has a high ion-exchange capacity, and charged amino acids are retained due to ion exchange mechanism and other mechanisms as well as partitioning, size exclusion, and adsorption [47]. In the classical usage with filling or polymeric columns the steady state of the ionic interactions is reached very fastly due to following the sample through the sorbent particles or polymeric mesh. In our particle separation the steady state is achieved after longer time because of big dilution of the

particles. When optimizing the incubation time there were observed the highest values of sarcosine bonding after 5 minutes. Between 10 and 30 minutes of incubation adsorption efficiency decreased. After 60 minutes lasting incubation amount of bounded sarcosine was approximately the same like after incubation for 30 minutes (Fig. 3C). The decreasing of the sarcosin interaction yield is belived to be associated with the electrostatic interactions between metal parts of the modified dowex coverage. Due to the observed maxima and its time progression fastly stopping of the incubation at 5minutes was crucial..

3.3.3 Optimization of the incubation temperature

To evaluate the temperature effect on the sarcosine adsorption efficiency the following temperatures as 1, 5, 10, 15, 20, 25, 30 and 35 °C were used (Fig. 3D). Lower temperatures showed the marked influence on adsorption of sarcosine to the surface of PMPs. As the most advantageous temperature for incubation 5 °C was found (Fig. 3D). This observation is in good agreement with the general statement that lower working temperatures enhance the efficiency of absorption of organic molecules to sorbent [48].

3.3.4 Optimization of the PMPs dose

The effect of doses of PMPs was examined with different concentrations of PMPs in 1 mL of water. The applied concentrations were 0.5; 1.5; 5; 10; 20; 40 and 60 $mg.mL^{-1}$ (Fig. 3E). Smaller particles should provide larger contact surface area for adsorption of analyte [44]. Our particles show a relatively large size (approximately 100 μm, refer to Fig. 2A) and adsorption exponentially increased to the highest dose used, namely 60 $mg.mL^{-1}$. There were also prepared saturation curves of 20, 40 and 60 $mg.mL^{-1}$ PMPs (Fig. 3F). Under applied concentration of PMPs of 20 $mg.mL^{-1}$, there was obtained linear dependence of sarcosine signal on the amount of the particles used ($y = 0.00108x + 0.716$, $R^2 = 0.9795$). It clearly

follows from the results obtained that saturation was increasing at concentration of PMPs 40 $mg.mL^{-1}$. For our purposes, the applied concentration 40 $mg.mL^{-1}$ ($y = 0.00122x + 0.6368$, $R^2 = 0.9955$) was selected, because it showed sufficient yield for isolation of sarcosine, because higher applied particle concentration 60 $mg.mL^{-1}$ provides not markedly better yield of sarcosine isolation ($y = 0.0031x + 0.047$; $R^2 = 0.9583$, Fig. 3F). Using the optimal conditions, we were able to estimated detection limit (3 S/N) of sarcosine as 1 μM when using PMPs.

3.4 Urine interferents

Urine is one of the most accessible and stable body fluids for metabolomics applications [49] however, urine volume and solute concentrations vary widely [50]. Nevertheless urine still acts as biological matrix containing interferents able to reduce the effectiveness of analytical assays. Thus we had to test the influence of common urine components on establishing the binding between sarcosine and PMPs.

3.4.1 Common urine components

After biochemical urine analysis substances with potential interference capability were selected (Figs. 4A-I). In Fig. 4A there are shown VIS peaks of sarcosine (1.1 mM) unbound, bound on PMPs and PMPs without sarcosine for comparison of retention times. It clearly follows from the results obtained that detected signals are well detected and separated (n = 10). Under the increasing concentrations (0.625; 1.25; 2.5; 5; 10 mM) of the components, Na^+ ions having the minimal influence on retention time of sarcosine had the highest effect on the capacity of particles to bind sarcosine (Fig. 4B and I). Further, creatinine had also considerable effect on the capacity and influenced the retention time of sarcosine (Fig. 4C and I). The effect of Na^+ ions is so marked due to the negative impact on the retention of the sarcosine on the column where it acts as eluent because Na^+ is replacing the NH_3^+ group of

the sarcosine on the active sulphuric group. The creatinine influence is caused by its higher isoelectric point (pI 8.47) against sarcosine (pI 7). That means the higher affinity of the creatinine molecule onto the ionex particle against the sarcosine, which results in the easing the sarcosin peak area (Fig. 4I). K^+ ions exhibited also the increased interference capability with a considerable moving of sarcosine retention time (Fig. 4D and I). Uric acid with no influence on retention time of sarcosine (Fig. 4E and I) and albumin also with no retention time impact (Fig. 4F and I) were tested. Low or no ability to influence capacity of the particles to bind sarcosine was detected at glucose with gentle moving of retention time to the right (Fig. 4G and I) and urea with no influence on sarcosine retention time (Fig. 4H and I). Based on the results obtained it can be concluded that Na^+ and K^+ and also creatinine mostly influence the binding of sarcosine on the surface of the particles probably mainly due to ionic interaction molecules. A significant effect of albumin is obvious due to its large molecule and affinity to different types of surfaces. Sugars are unlikely to have the effect of binding to the surface of the particles. Therefore, the suggested technology can be used for the isolation and characterization of sarcosine interferents within the concentration ranging from 2 to 4 mM.

3.4.2 Detection of sarcosine in urine

After analysis of interferents we carried out analysis of recovery of sarcosine from artificial urine and real urine sample. Artificial urine was made according to [51] and spiked with 1.1 mM of sarcosine. Retention time of sarcosine measured with and without using of PMPs in artificial urine was moving far to the left on the baseline. In real urine sample sarcosine retention was without significant changes (Fig. 5A). Recovery of sarcosine was measured in different dilutions of artificial urine with and without using of PMPs (Fig. 5B). Higher influence of dilutions was observed in real sample of urine, spiked with 1.1 mM of sarcosine (Fig. 5C). In both figures there are controls for comparison of recoveries. It clearly follows

from the results obtained that the interferents in the urine can strongly contribute to reducing the binding capacity of sarcosine to PMPs, as because recoveries with using PMPs are increasing with increasing dilution of urine. Nevertheless the dilution does not play a critical role for the usage of the flowthrough cell where the accumulation of the sarcosine could be proceeded continuously and thus we are not limited of negative effect of the Na^+ ions but only the creatinine or similar molecules with affinity onto the sulphuric group with higher affinity e.g. with higher isoelectric points or nonspecific binding.

4 Concluding remarks

Because of low fabrication cost, low material consumption, good analytical performance and the speed of analysis microfluidics has currently attracted much attention [52, 53]. Microfluidic systems have been widely recognized as a new emerging technology for the development of micro analytical systems, especially for bioassays [54-56], biochemical analysis and biosensors as well as chemical synthesis applications essentially require microfluidics for sample handling, treatment or readout [34, 39, 57-59]. Consideration for point-of-care devices in global diagnostics includes, among other factors, cost efficiency, ease-of-use and minimal requirements for infrastructure [60]. In this study, we developed a new microfluidic device that could be used for the isolation and determination of sarcosine as a potential prostate carcinoma marker. Usually used tests include examination per rectum, determination of prostate-specific antigen (PSA) levels and transrectal sonography with a biopsy of prostate tissue [61]. Due to the non-specifity of PSA and biopsy soreness determination of sarcosine in microchip could serve as a rapid, cheap and painless method.

There is also a number of advantages of using of the flow chip arrangement. It avoids the standard PMPs operational approaches as isolation with pipetting where the human factor is critical for the accuracy. Even the approaches using the automated pipetting stations are not

ideal because due to higher prize of the instrument and plastic material consumptions it is rather costs demanding and it also does not meet the Lab on chip philosophy. Contrary to this the broad availability, reliability, accuracy and the expensiveness is more convenient. Due these advantages the chip applications on the various backgrounds can serve as cheap alternative to the standard diagnostic approach.

Acknowledgement

Financial support by CEITEC CZ.1.05/1.1.00/02.0068, VSKE project and PGS01 2012 is highly acknowledged. The authors wish to express their thanks to Michal Zurek, Darina Maskova and Martina Stankova for perfect technical assistance.

Conflict of interest statement

The authors have declared no conflict of interest.

5 References

[1] Adamski, J., Suhre, K., *Curr. Opin. Biotechnol.* 2013, *24*, 39-47.

[2] Kwong, G. A., von Maltzahn, G., Murugappan, G., Abudayyeh, O., Mo, S., Papayannopoulos, I. A., Sverdlov, D. Y., Liu, S. B., Warren, A. D., Popov, Y., Schuppan, D., Bhatia, S. N., *Nat. Biotechnol.* 2013, *31*, 63-70.

[3] Zhang, A. H., Sun, H., Wu, X. H., Wang, X. J., *Clin. Chim. Acta* 2012, *414*, 65-69.

[4] Schulze, A., Harris, A. L., *Nature* 2012, *491*, 364-373.

[5] Sreekumar, A., Poisson, L. M., Rajendiran, T. M., Khan, A. P., Cao, Q., Yu, J. D., Laxman, B., Mehra, R., Lonigro, R. J., Li, Y., Nyati, M. K., Ahsan, A., Kalyana-Sundaram, S., Han, B., Cao, X. H., Byun, J., Omenn, G. S., Ghosh, D., Pennathur, S., Alexander, D. C.,

Berger, A., Shuster, J. R., Wei, J. T., Varambally, S., Beecher, C., Chinnaiyan, A. M., *Nature* 2009, *457*, 910-914.

[6] Jamaspishvili, T., Kral, M., Khomeriki, I., Student, V., Kolar, Z., Bouchal, J., *Prostate Cancer Prostatic Dis.* 2010, *13*, 12-19.

[7] Cavaliere, B., Macchione, B., Monteleone, M., Naccarato, A., Sindona, G., Tagarelli, A., *Anal. Bioanal. Chem.* 2011, *400*, 2903-2912.

[8] Petersen, L. F., Brockton, N. T., Bakkar, A., Liu, S. H., Wen, J., Weljie, A. M., Bismar, T. A., *BJU Int.* 2012, *109*, 788-795.

[9] Wagner, C., Luka, Z., *J. Urol.* 2011, *185*, 385-386.

[10] Armstrong, A. J., Eisenberger, M. A., Halabi, S., Oudard, S., Nanus, D. M., Petrylak, D. P., Sartor, A. O., Scher, H. I., *Eur. Urol.* 2012, *61*, 549-559.

[11] Lucarelli, G., Fanelli, M., Larocca, A. M. V., Germinario, C. A., Rutigliano, M., Vavallo, A., Selvaggi, F. P., Bettocchi, C., Battaglia, M., Ditonno, P., *Prostate* 2012, *72*, 1611-1621.

[12] Jentzmik, F., Stephan, C., Miller, K., Schrader, M., Erbersdobler, A., Kristiansen, G., Lein, M., Jung, K., *Eur. Urol.* 2010, *58*, 12-18.

[13] Cernei, N., Zitka, O., Ryvolova, M., Adam, V., Masarik, M., Hubalek, J., Kizek, R., *Int. J. Electrochem. Sci.* 2012, *7*, 4286-4301.

[14] Cernei, N., Zitka, O., Skalickova, S., Gumulec, J., Sztalmachova, M., Merlos Rodrigo, M. A., Sochor, J., Masarik, M., Adam, V., Hubalek, J., Trnkova, L., Kruseova, J., Eckschlager, T., Kizek, R., *Oncol. Rep.* 2013, *in press*.

[15] Guo, W. P., Fung, Y. S., *Electrophoresis* 2011, *32*, 3437-3445.

[16] Li, Y. Y., Zhang, Y., Qiu, F., Qiu, Z. Y., *Electrophoresis* 2011, *32*, 1976-1983.

[17] Lindenburg, P. W., Tjaden, U. R., van der Greef, J., Hankemeier, T., *Electrophoresis* 2012, *33*, 2987-2995.

[18] Ramautar, R., Torano, J. S., Somsen, G. W., de Jong, G. J., *Electrophoresis* 2010, *31*, 2319-2327.

[19] Wu, R. G., Yeung, W. S. B., Fung, Y. S., *Electrophoresis* 2011, *32*, 3406-3414.

[20] Jiang, Y. Q., Cheng, X. L., Wang, C. A., Ma, Y. F., *Anal. Chem.* 2010, *82*, 9022-9027.

[21] Jentzmik, F., Stephan, C., Lein, M., Miller, K., Kamlage, B., Bethan, B., Kristiansen, G., Jung, K., *J. Urol.* 2011, *185*, 706-711.

[22] Issaq, H. J., Waybright, T. J., Veenstra, T. D., *Electrophoresis* 2011, *32*, 967-975.

[23] Wu, H., Liu, T. T., Ma, C. G., Xue, R. Y., Deng, C. H., Zeng, H. Z., Shen, X. Z., *Anal. Bioanal. Chem.* 2011, *401*, 635-646.

[24] Meyer, T. E., Fox, S. D., Issaq, H. J., Xu, X., Chu, L. W., Veenstra, T. D., Hsing, A. W., *Anal. Chem.* 2011, *83*, 5735-5740.

[25] Gamagedara, S., Ma, Y. F., *Bioanalysis* 2011, *3*, 2129-2142.

[26] Bianchi, F., Dugheri, S., Musci, M., Bonacchi, A., Salvadori, E., Arcangeli, G., Cupelli, V., Lanciotti, M., Masieri, L., Serni, S., Carini, M., Careri, M., Mangia, A., *Anal. Chim. Acta* 2011, *707*, 197-203.

[27] Soliman, L. C., Hui, Y., Hewavitharana, A. K., Chen, D. D. Y., *J. Chromatogr. A* 2012, *1267*, 162-169.

[28] Chen, J., Zhou, L. N., Zhang, X. Y., Lu, X., Cao, R., Xu, C. J., Xu, G. W., *Electrophoresis* 2012, *33*, 3361-3369.

[29] Sezginturk, M. K., Dinckaya, E., *Prep. Biochem. Biotechnol.* 2011, *41*, 30-39.

[30] Narakathu, B. B., Atashbar, M. Z., Bejcek, B. E., *Biosens. Bioelectron.* 2010, *26*, 923-928.

[31] Zhou, Y. L., Yin, H. S., Meng, X. M., Xu, Z. N., Fu, Y. R., Ai, S. Y., *Electrochim. Acta* 2012, *71*, 294-301.

[32] Pamme, N., *Curr. Opin. Chem. Biol.* 2012, *16*, 436-443.

[33] Ng, A. H. C., Choi, K., Luoma, R. P., Robinson, J. M., Wheeler, A. R., *Anal. Chem.* 2012, *84*, 8805-8812.

[34] Adam, V., Huska, D., Hubalek, J., Kizek, R., *Microfluid. Nanofluid.* 2010, *8*, 329-339.

[35] Magro, M., Sinigaglia, G., Nodari, L., Tucek, J., Polakova, K., Marusak, Z., Cardillo, S., Salviulo, G., Russo, U., Stevanato, R., Zboril, R., Vianello, F., *Acta Biomater.* 2012, *8*, 2068-2076.

[36] Prucek, R., Tucek, J., Kilianova, M., Panacek, A., Kvitek, L., Filip, J., Kolar, M., Tomankova, K., Zboril, R., *Biomaterials* 2011, *32*, 4704-4713.

[37] Liljeroth, P., Johans, C., Slevin, C. J., Quinn, B. M., Kontturi, K., *Electrochem. Commun.* 2002, *4*, 67-71.

[38] Wittstock, G., *Fresenius J. Anal. Chem.* 2001, *370*, 303-315.

[39] Waldbaur, A., Rapp, H., Lange, K., Rapp, B. E., *Anal. Methods* 2011, *3*, 2681-2716.

[40] Cernei, N., Masarik, M., Gumulec, J., Zitka, O., Babula, P., Kizek, R., *J. Biochem. Techol.* 2010, *2*, S7-S8.

[41] Causon, R., *J. Chromatogr. B* 1997, *689*, 175-180.

[42] Bugianesi, R., Serafini, M., Simone, F., Wu, D. Y., Meydani, S., Ferro-Luzzi, A., Azzini, E., Maiani, G., *Anal. Biochem.* 2000, *284*, 296-300.

[43] Long, G. L., Winefordner, J. D., *Anal. Chem.* 1983, *55*, A712-A724.

[44] Zhang, X. C., Xie, S. P., Paau, M. C., Zheng, B. Z., Yuan, H. Y., Xiao, D., Choi, M. M. F., *J. Chromatogr. A* 2012, *1247*, 1-9.

[45] Cheng, S. L., Yan, H. S., Zhao, C. Q., *J. Chromatogr. A* 2006, *1108*, 43-49.

[46] Echigo, T., Aruguete, D. M., Murayama, M., Hochella, M. F., *Geochim. Cosmochim. Acta* 2012, *90*, 149-162.

[47] Rigas, P. G., *Instrum. Sci. Technol.* 2012, *40*, 161-193.

[48] Moreno-Castilla, C., *Carbon* 2004, *42*, 83-94.

[49] Ryan, D., Robards, K., Prenzler, P. D., Kendall, M., *Anal. Chim. Acta* 2011, *684*, 17-29.

[50] Mattarucchi, E., Guillou, C., *Biomed. Chromatogr.* 2012, *26*, 512-517.

[51] Brooks, T., Keevil, C. W., *Lett. Appl. Microbiol.* 1997, *24*, 203-206.

[52] Li, S., Li, M., Hui, Y. S., Cao, W., Li, W., Wen, W., *Microfluid. Nanofluid.* 2013, *14*, 499-508.

[53] Gaspar, A., Salgado, M., Stevens, S., Gomez, F. A., *Electrophoresis* 2010, *31*, 2520-2525.

[54] Liu, K.-K., Wu, R.-G., Chuang, Y.-J., Khoo, H. S., Huang, S.-H., Tseng, F.-G., *Sensors* 2010, *10*, 6623-6661.

[55] Arce, C. L., Witters, D., Puers, R., Lammertyn, J., Bienstman, P., *Anal. Bioanal. Chem.* 2012, *404*, 2887-2894.

[56] Zitka, O., Krizkova, S., Krejcova, L., Hynek, D., Gumulec, J., Masarik, M., Sochor, J., Adam, V., Hubalek, J., Trnkova, L., Kizek, R., *Electrophoresis* 2011, *32*, 3207-3220.

[57] Huska, D., Adam, V., Babula, P., Trnkova, L., Hubalek, J., Zehnalek, J., Havel, L., Kizek, R., *Microchim. Acta* 2011, *173*, 189-197.

[58] Adam, V., Zitka, O., Dolezal, P., Zeman, L., Horna, A., Hubalek, J., Sileny, J., Krizkova, S., Trnkova, L., Kizek, R., *Sensors* 2008, *8*, 464-487.

[59] Zitka, O., Krizkova, S., Skalickova, S., Dospivova, D., Adam, V., Kizek, R., *Electrophoresis* 2013, *in press*.

[60] Godino, N., Gorkin, R., Bourke, K., Ducree, J., *Lab Chip* 2012, *12*, 3281-3284.

[61] Prensner, J. R., Rubin, M. A., Wei, J. T., Chinnaiyan, A. M., *Sci. Transl. Med.* 2012, *4*, 1-11.

Figure 1

Pictures of PMPs obtained with electron microscope. (**Aa**) Picture of two Dowex beads, covered with Fe_2O_3 nanoparticles. (**Ab**) Detail of one Dowex particle, covered with Fe_2O_3 nanoparticles. (**Ac**) Red highlighted iron from Fe_2O_3 nanoparticles makes partial cover of the Dowex bead. (**Ad**) Orange highlighted SO_3^- groups belong to the surface of Dowex bead and mediate the binding of sarcosine. Scans of PMPs by electrochemical microscope. (**Ba**) Vertical scan of relative current response of bead without sarcosine. (**Bb**) Vertical scan of relative current response of bead with sarcosine bound. Other experimental details are in Captions 2.3 and 2.4.

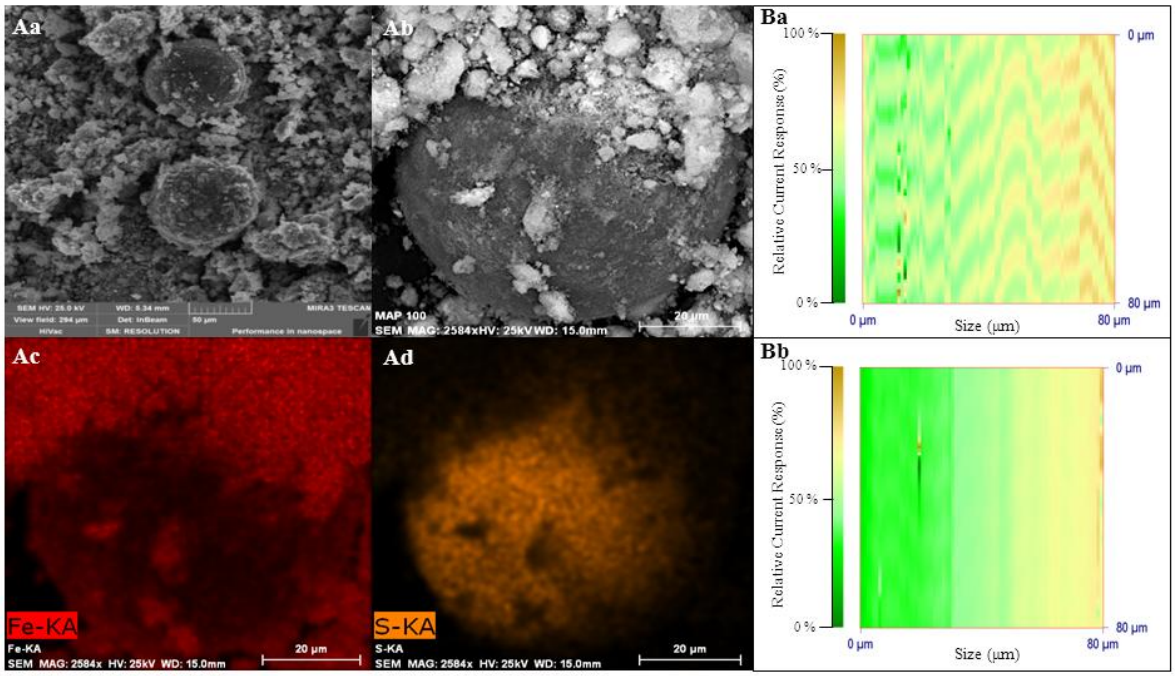

Figure 1

Figure 2

Scheme of the microfluidic system for sarcosine isolation with sections for (**A**) sample inlet, (**B**) binding buffer inlet, (**C**) rinsing buffer inlet, (**D**) paramagnetic particles inlet, (**E**) output for elution of analyte. The mixing of the particles is due to (**F**) moving permanent magnet on the (**G**) bottom of the chip holder. Other experimental details are in Caption 2.5.

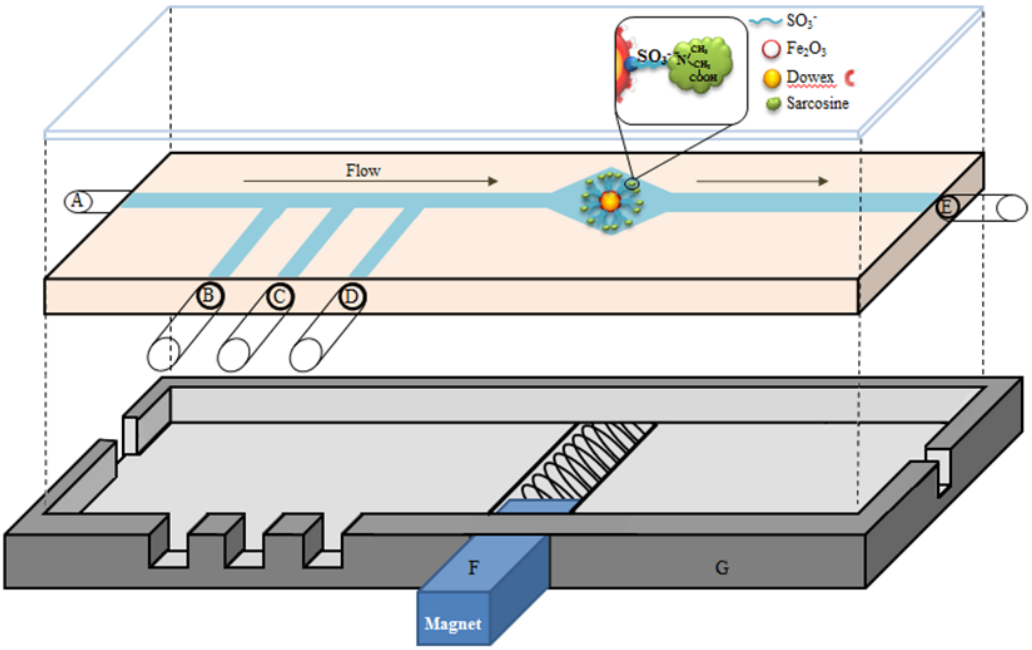

Figure 2

Figure 3

(**A**) Workflow scheme of sarcosine isolation with PMPs. PMPs were washed with PBS buffer, then in Britton-Robinson (B-R) buffer. In the following step a binding of sarcosine from sample with PMPs was established and incubation followed. After incubation there was included another washing step in B-R buffer and retentate was removed to 96-well evaporation plate and dissolved in HCl. This mixture was incubated for perfect dissolution and evaporated. Evaporated concentrate was resuspended in dilution buffer and analysed using AAA. All optimizing steps of sarcosine isolation were carried out with constant concentration of sarcosine of 1.1 mM. Dependences of sarscosine signal after isolation on (**B**) pH conditions (Britton-Robinson buffer ranging pH 2 - 4), (**C**) time and (**D**) temperature. (**E**) Saturation curves of different concentrations of Fe_2O_3 microparticles and (**F**) calibration curves made from three points of saturation curves. Other experimental details are in Caption 2.6.

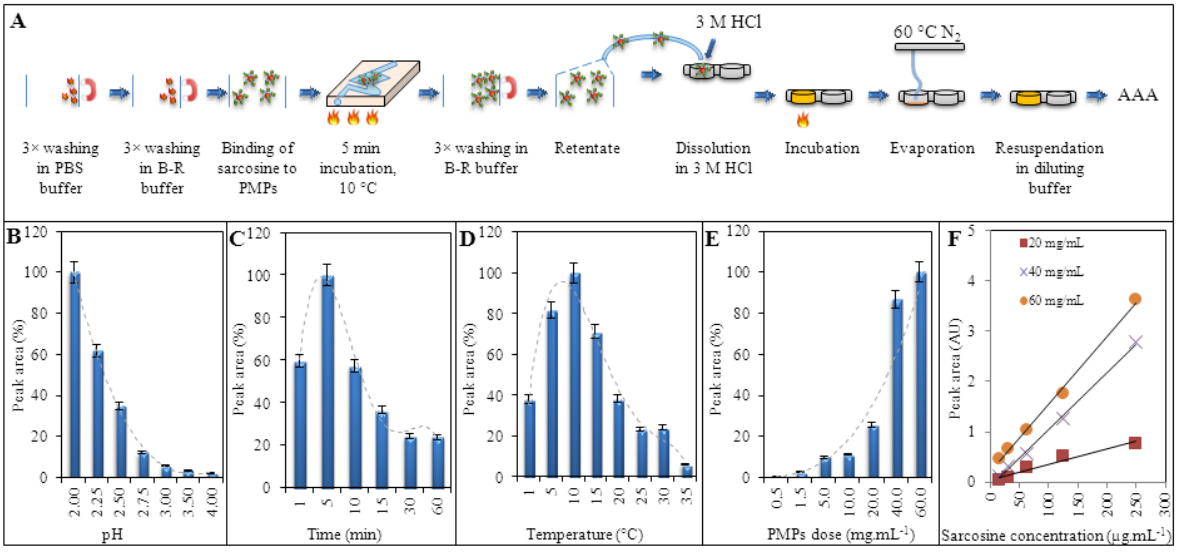

Figure 3

Figure 4

(**A**) Overlay of chromatograms of sarcosine standard, sarcosine isolated by PMPs and blank PMPs without the addition of sarcosine. All interferents chromatograms were carried out with sarcosine concentration of 1 $mg.mL^{-1}$. Chromatograms of sarcosine from testing of interferents (concentration of all interferent compounds was 1.25 mM) under influence of (**B**) NaCl, (**C**) creatinine, (**D**) KCl, (**E**) uric acid, (**F**) albumin, (**G**) glucose and (**H**) urea. (**I**) Overall influence of the concentrations of common urine components (0.625; 1.25; 2.5; 5 and 10 mM) on sarcosine-PMPs binding expressed as peak area. Concentration of sarcosine was 1.1 mM. Other experimental details are in Captions 2.7 and 2.8.

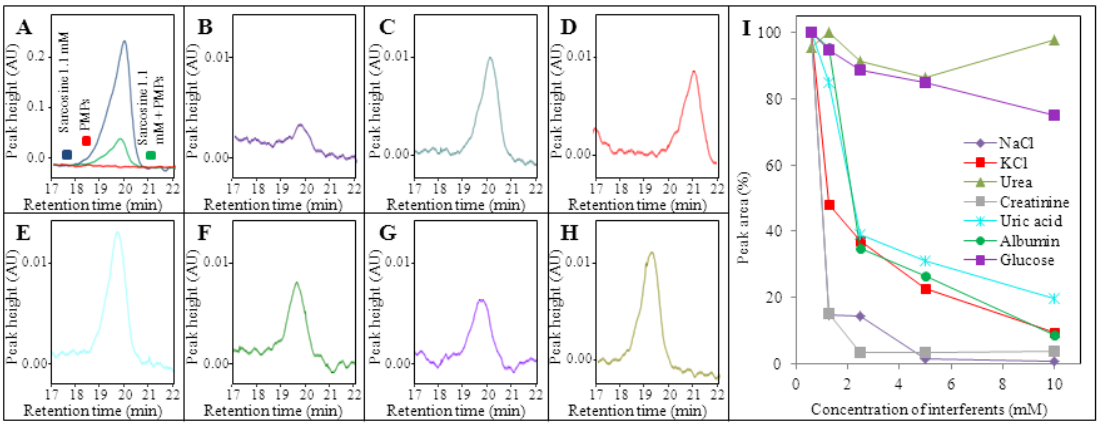

Figure 4

Figure 5

(**A**) Overlay of chromatograms of sarcosine spike (concentration 1.1 mM) and influence of with and without using of PMPs in artificial and real urine diluted 50 times on sarcosine retention times. Sarcosine (concentration 1.1 mM) recovery in different dilutions gained from: (**B**) artificial urine and (**C**) real urine. Both figures contain control measuring of sarcosine unbound and bound with PMPs for comparison of sarcosine recovery. Other experimental details are in Captions 2.7 and 2.8.

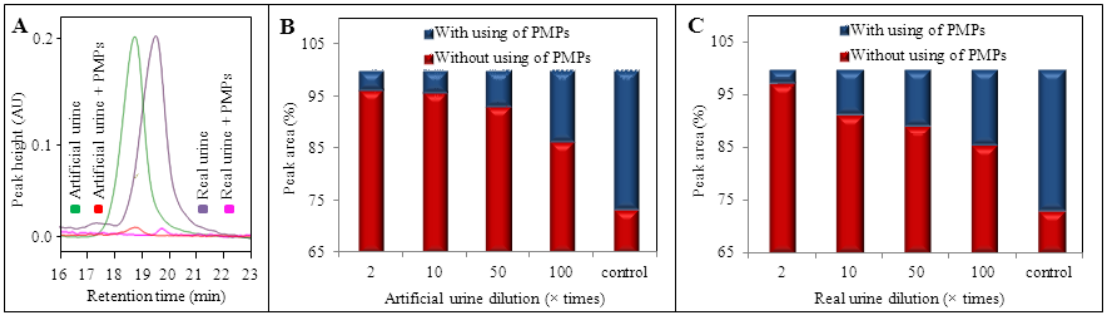

Figure 5